Journal of Physics: Conference Series **137** (2008) 012029 doi:10.1088/1742-6596/137/1/012029

# Statistical analysis of the transition to turbulent-laminar banded patterns in plane Couette flow

**Laurette S. Tuckerman**

PMMH-ESPCI (UMR 7636, CNRS, Univ. Paris 6 & 7), 10 rue Vauquelin, 75231 Paris, France

E-mail: laurette@pmmh.espci.fr

**Dwight Barkley**

Mathematics Institute and Centre for Scientific Computing, University of Warwick, Coventry CV4 7AL, United Kingdom

E-mail: D.Barkley@warwick.ac.uk

**Olivier Dauchot**

CEA-Saclay, SPEC-GIT, URA 2464, 91191 Gif-sur-Yvette, France

E-mail: dauchot@cea.fr

**Abstract.** The transition between uniform turbulence in plane Couette flow and turbulent-laminar banded patterns is studied using numerical computations. Timeseries of the velocity along a line in the midplane along the pattern wavevector are Fourier transformed. When averaged in time, these spectra show diffuse maxima corresponding to streaks and longitudinal rolls with a wavelength near 4, and a sharper, higher, maximum corresponding to the turbulent-laminar pattern with wavelength 40. Probability distribution functions are computed for the Fourier component corresponding to wavelength 40. It is shown that this PDF is a Gaussian centered at 0 for a a uniform turbulent flow and that this maximum shifts to a finite value when a turbulent-laminar banded pattern appears.

In large-aspect-ratio plane Couette flow, a pattern of oblique bands, alternating between turbulent and laminar flow, is the intermediate regime between uniform turbulence and simple laminar flow [1, 2]. The pattern wavelength is much larger than the gap and the pattern wavevector is oriented obliquely to the streamwise direction; typical values are 40 half-gaps and 24°. We have reproduced and studied these patterns numerically [3] in fully resolved simulations of the Navier-Stokes equations. Here, we focus on the *transition* between uniform turbulence and the turbulent-laminar pattern.

Figure 1 shows a perspective plot of one of our computed turbulent-laminar patterned flows. Our computations use a horizontally periodic domain whose length (in the $z$ direction) is the expected pattern wavelength and whose orientation is along the expected pattern wavevector. Figure 2 illustrates our computational domain. Within this domain, we use a spectral element-Fourier code [4], with $N_x \times N_y \times N_z = 81 \times 41 \times 512$ points or modes to resolve a domain of size $L_x \times L_y \times L_z = 10 \times 2 \times 40$. In our previous research [5], we have shown that the mean flows corresponding to these patterns are represented almost perfectly by a single trigonometric

 

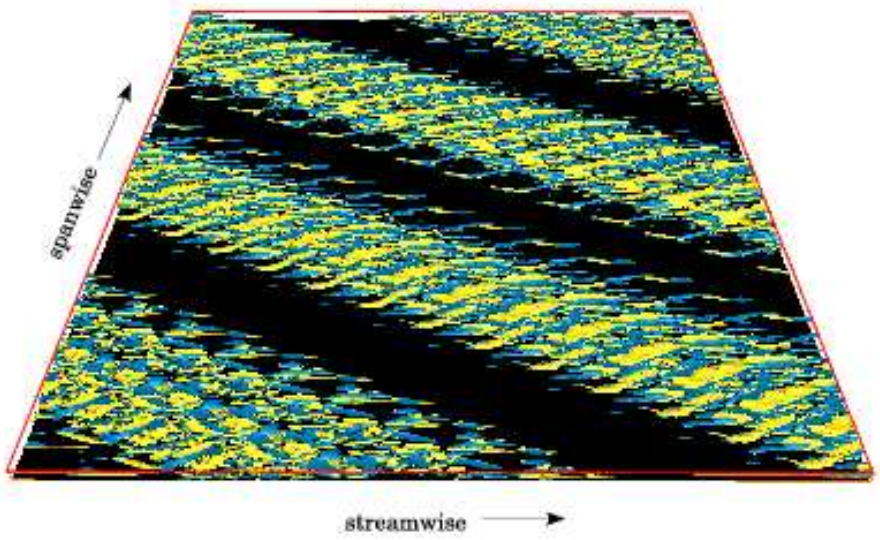


**Figure 1.** Turbulent-laminar pattern at Reynolds number 350. Isosurfaces of instantaneous streamwise vorticity. This visualization is constructed by tiling a large domain with many repetitions of our computational domain.

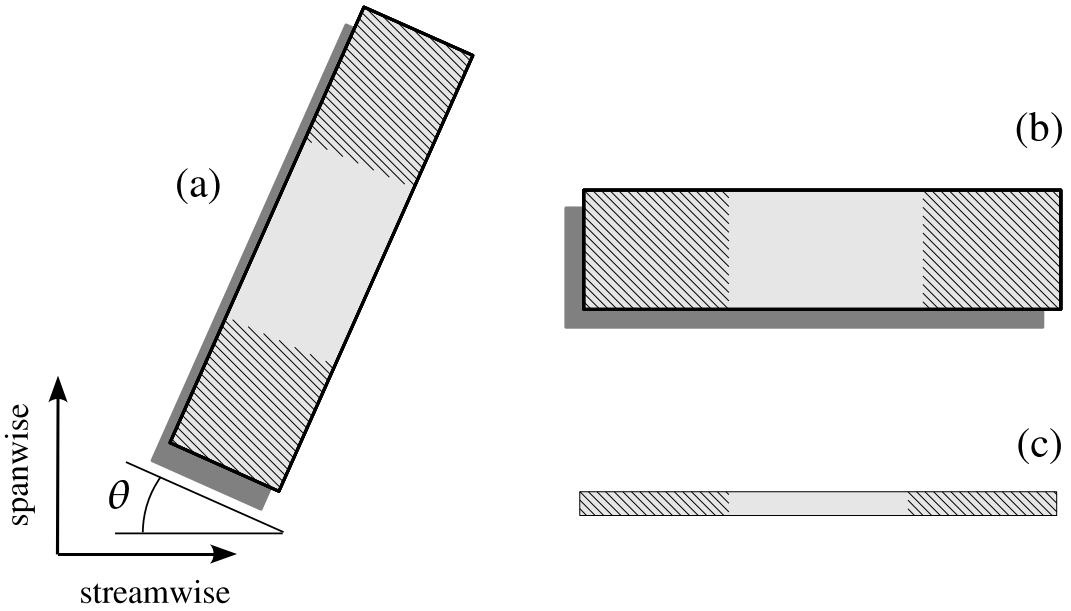


**Figure 2.** Computational domain oriented at angle $\theta$ to the streamwise-spanwise directions. The $z$ direction is aligned to the pattern wavevector. The turbulent region is represented schematically by hatching. (a) Domain oriented with streamwise velocity horizontal, as in figure 1. (b) Domain oriented with $z$ horizontal, as in remainder of paper. (c) View between the plates.

function along the direction of the pattern wavevector, which we denote by $z$. The Fourier component corresponding to the pattern wavelength thus provides an order parameter for the transition. Here we will analyse the dependence of this Fourier component and its statistical properties on the Reynolds number.

The data we analyze are timeseries of the velocity at 32 equally spaced values of $z$ along a line $x = y = 0$ in the mid-plane. In the first row of figure 3, we show timeseries of the spanwise velocity for a turbulent-laminar pattern at $Re = 350$, an intermittent state at $Re = 410$ and a state at $Re = 500$ in which the turbulence is uniform in the $z$ direction. In this investigation, a single timeseries is analyzed for each value of $Re$. We then take the modulus of the Fourier transform in the $z$ direction of this data. The time-average of the square modulus of the Fourier transform, i.e. the power spectrum $\mathrm{avg}(|\mathrm{span}_m|^2)$, of the spanwise velocity is shown in the second row of figure 3. These spanwise spectra show very little variation with the wavenumber $m$, except for one very prominent feature: the $m = 1$ Fourier component corresponding to wavelength 40 and shown as a blue square emerges from the rest of the spectrum at $Re = 350$ and, to a lesser extent, at $Re = 410$. The corresponding power spectra of the streamwise velocity $\mathrm{avg}(|\mathrm{strm}_m|^2)$ are shown in the third row of figure 3. In addition to the peak at $m = 1$, the spectra of the streamwise velocity also display a broad peak at $7 \lesssim m \lesssim 11$, corresponding to wavelengths 3.6–5.7 and shown as red triangles. This peak reflects the streamwise streaks, i.e. the spanwise variation of the streamwise velocity which are the "texture" of wall-bounded turbulence. These streaks are intimately connected with longitudinal vortices which rotate in the cross-channel and spanwise plane. The absence of these peaks in the spanwise spectra implies that these vortices are centered between the plates and so the velocity in the midplane is exclusively in the cross-channel direction. Indeed, spectra of the cross-channel velocity $\mathrm{avg}(|\mathrm{cross}_m|^2)$ show the broad peaks corresponding to the streaks and not the $m = 1$ peak corresponding to the pattern. Using the color coding above, we can combine the spectra, which we display as a function of Reynolds number in figure 4.

We now consider the distribution of values of the modulus $a$ of the $m = 1$ Fourier component of the spanwise velocity $\mathrm{span}_1$ corresponding to the turbulent-laminar pattern. Writing $\mathrm{span}_1 = a\exp(i\phi)$, the probability distribution $p(a, \phi)$ satisfies

$$1 = \int_0^\infty a da \underbrace{\int_0^{2\pi} d\phi\, p(a,\phi)}_{p(a)} \tag{1}$$

By counting the occurrences of $a$ within the interval $[a_i, a_{i+1}]$, we estimate

$$\int_{a_i}^{a_{i+1}} a da \int_0^{2\pi} d\phi\, p(a,\phi) \tag{2}$$

Dividing (2) by $(a_{i+1} - a_i)(a_i + a_{i+1})/2$ leads to an approximation of $p(a)$ at $(a_i + a_{i+1})/2$.

The probability density functions for various Reynolds numbers are shown on the left part of figure 5. For $Re \geq 440$, when the turbulence is uniform, the maximum, i.e. the most probable value, is at $a_{\max} = 0$ and

$$\ln p(a) = c_0 + c_2 a^2 \tag{3}$$

provides an excellent fit, i.e. $p(a)$ is almost perfectly Gaussian. As shown in figure 5, the most probable value shifts to positive $a$ as $Re$ is lowered and a pattern appears. Generalizing (3) to a functional form which fits $p(a)$ for lower values of $Re$ has thus far proved to be problematic. The canonical scenario would include a quartic term $c_4 a^4$ in (3) ; $c_4$ would vary little with $Re$ while $c_2$ would change sign at the transition. However, addition of $c_4 a^4$ does not provide a good fit for any of the patterned flows, as exemplified by the dashed blue curve of figure 5 for $Re = 350$.

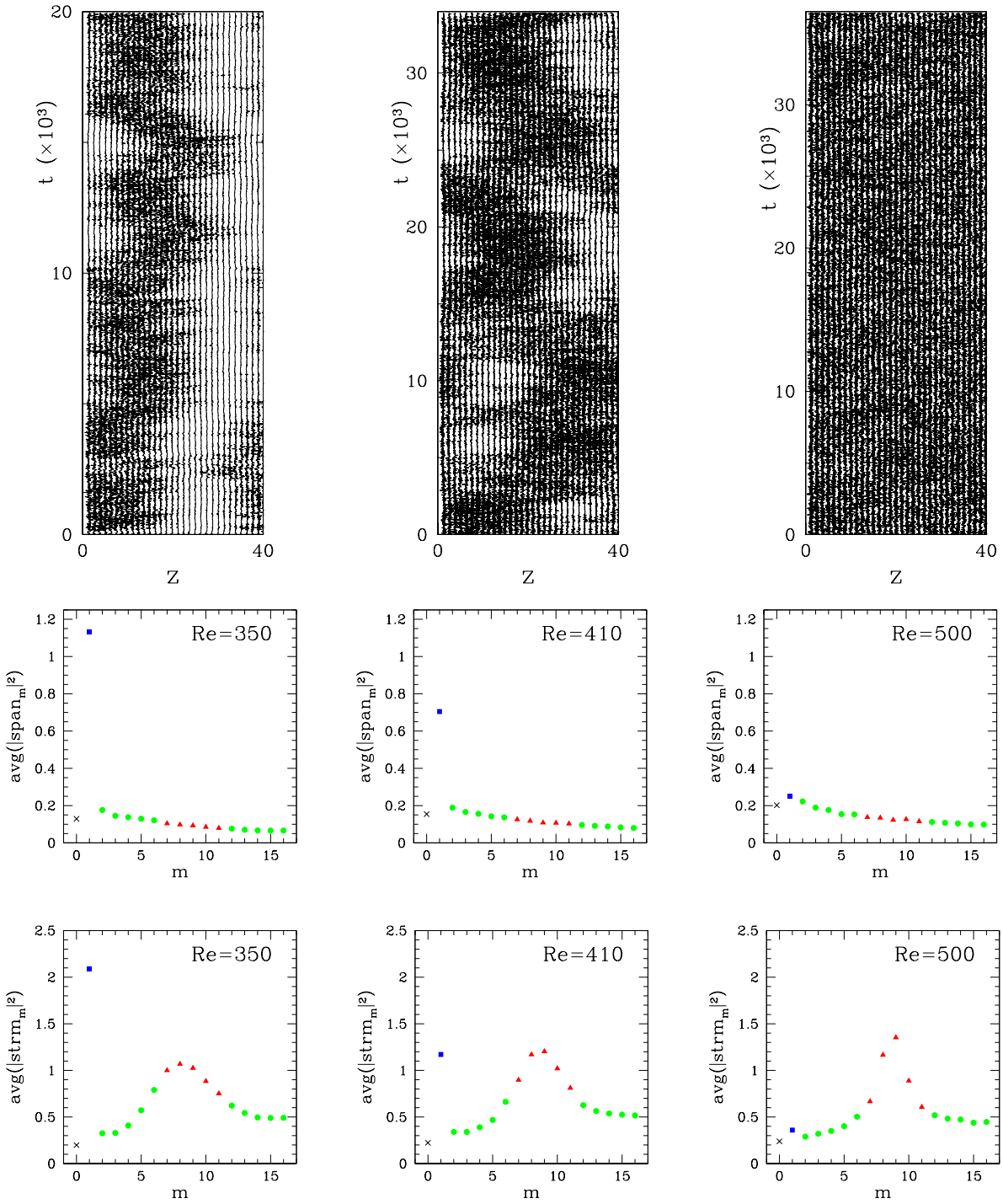


**Figure 3.** Left column: statistically steady turbulent-laminar pattern at $Re = 350$. Middle column: intermittent state at $Re = 410$. Right column: uniform turbulence at $Re = 500$. Top row: timeseries of the spanwise velocity along the line $x = y = 0$ at 32 equally spaced values of $z$. Middle row: time-average of the power spectrum in $z$ of the spanwise velocity. Bottom row: time-average of the power spectrum of the streamwise velocity. The blue square at $m = 1$ corresponds to the pattern wavelength of 40. The red triangles at $7 \lesssim m \lesssim 11$ correspond to streaks of wavelength near 40/9=4.44. The $m = 0$ component is shown as a black cross and the remaining components are shown as green dots.

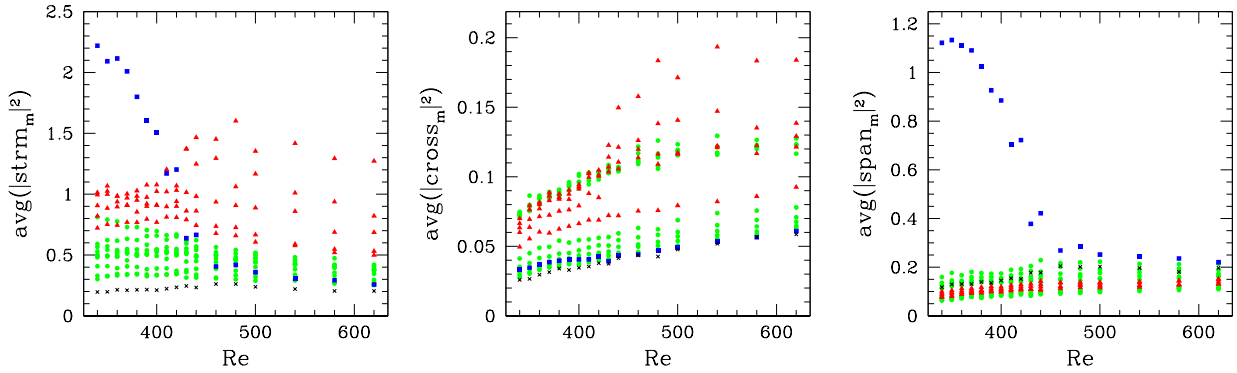


**Figure 4.** Power spectra as a function of $Re$. Left: streamwise. Middle: cross-channel. Right: spanwise. Blue squares: wavenumber $m = 1$ corresponding to pattern wavelength 40. Red triangles: wavenumbers $7 \lesssim m \lesssim 11$ corresponding to streaks of wavelengths near 40/9=4.44. Black crosses: wavenumber $m = 0$. Green dots: other wavenumbers. Transition involves both $m = 1$ mode (blue square, higher for $Re < Re_c$) and streak modes (red triangles, higher for $Re > Re_c$). Streamwise spectrum shows transition in both pattern and streaks. Cross-channel spectrum shows only streaks transition. Spanwise spectrum shows pattern transition most clearly.

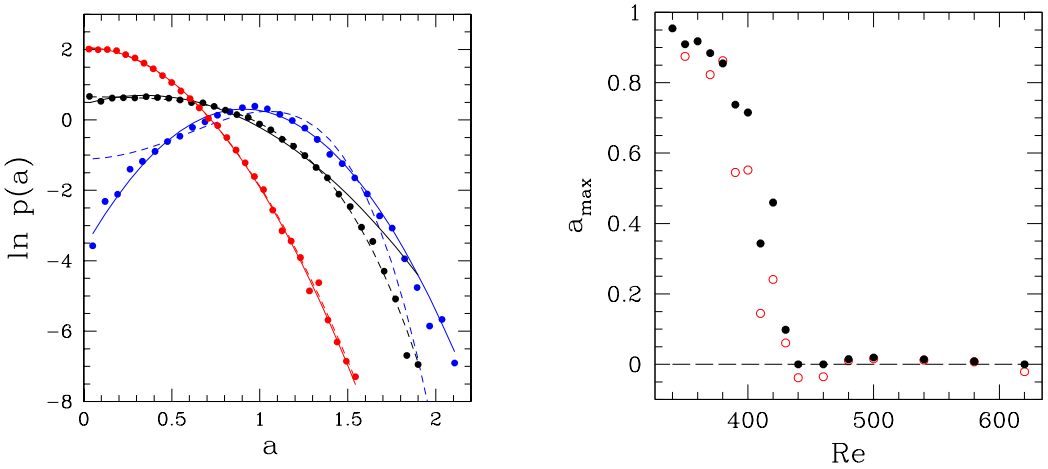


**Figure 5.** Left: probability distribution functions $p(a)$ for $Re = 500$ (red, highest at $a = 0$), $Re = 410$ (black), and $Re = 350$ (blue, lowest at $a = 0$). Points indicate values obtained by postprocessing full numerical simulations. PDFs for uniform turbulent states are all quantitatively, as well as qualitatively similar; PDFs for turbulent-laminar patterns are also similar. Solid curves are least-squares fits to the functional form $\ln p(a) = c_0 + c_1 a + c_2 a^2$, with the weighting function $p(a)$; dashed curves are least-squares fit to the functional form $\ln p(a) = c_0 + c_2 a^2 + c_4 a^4$. Right: Maximum $a_{\max}$ of PDFs as a function of Reynolds number (solid black dots) and coefficient $c_1/10$ (hollow red dots) from least-squares fit.

A better fit is provided by including instead a linear term $c_1 a$, as shown by the solid blue curve. This functional form gives $a_{\max} = -c_1/(2c_2)$ as the most probable value. Both $a_{\max}$ and $c_1$ are shown on the right part of figure 5. When $Re \leq 460$, $p(a)$ begins to widen and when $Re \leq 440$, $a_{\max}$ is no longer zero.

We have shown that turbulent-laminar patterns in plane Couette flow are well-characterized by their Fourier spectra along the direction of the pattern wavevector. The spectrum distinguishes small-scale structures, notably streaks, and also the large-scale pattern. The amplitude of the Fourier component corresponding to the pattern provides an excellent order parameter for the transition from uniform turbulence. Future plans include the analysis of multiple timeseries at each value of $Re$, in order to acquire more accurate information about the PDFs, particularly their tails.

## Acknowledgments

The simulations analyzed in this work were performed on the IBM Power 4 of the IDRIS-CNRS supercomputing center as part of project 1119.

## References

[1] Prigent A, Grégoire G, Chaté H, Dauchot O and van Saarloos W 2002, Large-scale finite-wavelength modulation within turbulent shear flows, *Phys. Rev. Lett.* **89**, 014501
[2] Prigent A, Grégoire G, Chaté and Dauchot O 2003, Long-wavelength modulation of turbulent shear flows, *Physica D* **174**, 100
[3] Barkley D and Tuckerman L S 2005, Computational study of turbulent laminar patterns in Couette flow, Phys. Rev. Lett. **94**, 014502
[4] Henderson R D and Karniadakis G E 1995, Unstructured spectral element methods for simulation of turbulent flows, *J. Comput. Phys.* **122**, 191–217
[5] Barkley D and Tuckerman L S 2007, Mean flow of turbulent-laminar patterns in plane Couette flow, *J. Fluid Mech.* **576**, 109–137